Chaperon-Mediated Single Molecular Approach Toward Modulating Aβ Peptide Aggregation

ARTICLE *in* NANO LETTERS · OCTOBER 2009

Impact Factor: 13.59 · DOI: 10.1021/nl902256b · Source: PubMed

NANO LETTERS

2009
Vol. 9, No. 12
4066-4072

Chaperon-Mediated Single Molecular Approach Toward Modulating Aβ Peptide Aggregation

Lei Liu, Lan Zhang, Xiaobo Mao, Lin Niu, Yanlian Yang,* and Chen Wang*

National Center for Nanoscience and Technology Beijing 100190, China

Received July 14, 2009; Revised Manuscript Received September 14, 2009

ABSTRACT

We report here a single molecular approach using chaperone-like molecular modulators for modulating the aggregation behavior of a vital analogue of beta-amyloid peptide (Aβ) by using scanning tunneling microscopy. The molecular structures of the β-sheets for Aβ33−42 peptide are revealed, which are keen to the aggregation of Aβ42 relating to Alzheimer's disease. It was identified that the introduction of chaperone-like modulators could regulate the assembling behavior of the peptide at molecular level. Furthermore, the modulators could also significantly accelerate the aggregation of the peptide in aqueous solution as revealed by light scattering studies. These observations of the molecular modulator effect in peptide assemblies could provide a novel approach toward modulating Aβ peptide aggregations.

Alzheimer's disease (AD) is a neurodegenerative disease[1] related to beta-amyloid peptide (Aβ) derived from the amyloid precursor protein (APP) by proteolysis. Different proteolytic products have been reported depending on the proteolytic processes in which APP may be incised to form Aβ42, Aβ40, and Aβ(1 − x) etc.[2−4] These proteolytic products are all considered relevant to the pathogenesis of AD disease. Reports from extensive studies have elucidated that beta amyloid peptides and other amyloidogenic proteins could form diversity of aggregate morphologies, such as nanofibrils[5] (7−12 nm in diameter), spherical aggregates[6] (5−6 nm in size), annular protofibirils,[7] and nanopore-like structures with lipid membrane[8] (outer diameter 8−12 nm; inner diameter 2.0−2.5 nm). These aggregates with a variety of nanostructures are all reported to be correlated to neurotoxicity at different levels[6,8,9] and the nanopore-like aggregates of various amyloid peptides on membrane result in cellular calcium loading leading to dysfunction and degeneration of the cells.[8] In addition, several reports[10,11] revealed that Aβ28, an analogue of Aβ42, could also form fibrils in vitro which are similar to the in vivo amyloid aggregates of large bundles resembling the senile plaque cores. Reports also suggested that Aβ25−35, a fragment of Aβ42, could form oligomers and proto-fibrils and could be neurotoxic to cells.[12−15] It is therefore plausible to consider that a variety of peptide fragments could be related to Alzheimer's disease. However, it is still challenging to fully understand the aggregation process of the peptides that are vital for early stage diagnosis and treatment of amyloidosis, due to the lacking of high resolution structural analysis of peptide aggregates.

Many techniques have been applied to investigate the aggregation mechanisms of amyloid peptides represented by Aβ42.[2−4,16,17] As the examples, electron microscopy,[18,19] solid-state NMR spectroscopy,[20−22] and X-ray diffraction[23,24] have been utilized to investigate the structural information of Aβ42 aggregates and the Aβ fragments.[25−27] It is known that the lamella assemblies of Aβ42 hairpin have two sides, namely two peptide fragments consisting of amino acids with sequences of 33−42 and 10−20.[21] The reported NMR studies[21,22] suggested that Aβ lamella structure consists exclusively of hairpins with parallel configuration, while other reports suggested the antiparallel configuration.[28,29] Scanning probe microscopy (SPM), represented by scanning tunneling microscopy (STM) and atomic force microscopy (AFM), has proved to be a powerful tool for studying organic and biological species at molecular or submolecular levels due to its high structural resolution and adaptability to various environments including liquid−solid interfaces[30] and ultra-high-vacuum (UHV) conditions.[31] Recently, STM technique has been applied to study the submolecular structure of diphenylalanine peptide in UHV system,[32] and also the assembling characteristics of Aβ42 lamellae[33] at liquid−solid interface. These progresses provide possibilities for using STM to study the assembly structures of amyloid peptide with high structural resolution that could be complementary to structural analysis by other methods.

In this work, we investigated the assembling behavior of Aβ33−42 peptide, which is the key sequence for the formation of the hairpin structure in Aβ42 lamella as-

* To whom correspondence should be addressed. E-mail: (C.W.) wangch@nanoctr.cn; (Y.Y.) yangyl@nanoctr.cn.

10.1021/nl902256b CCC: $40.75
Published on Web 10/20/2009

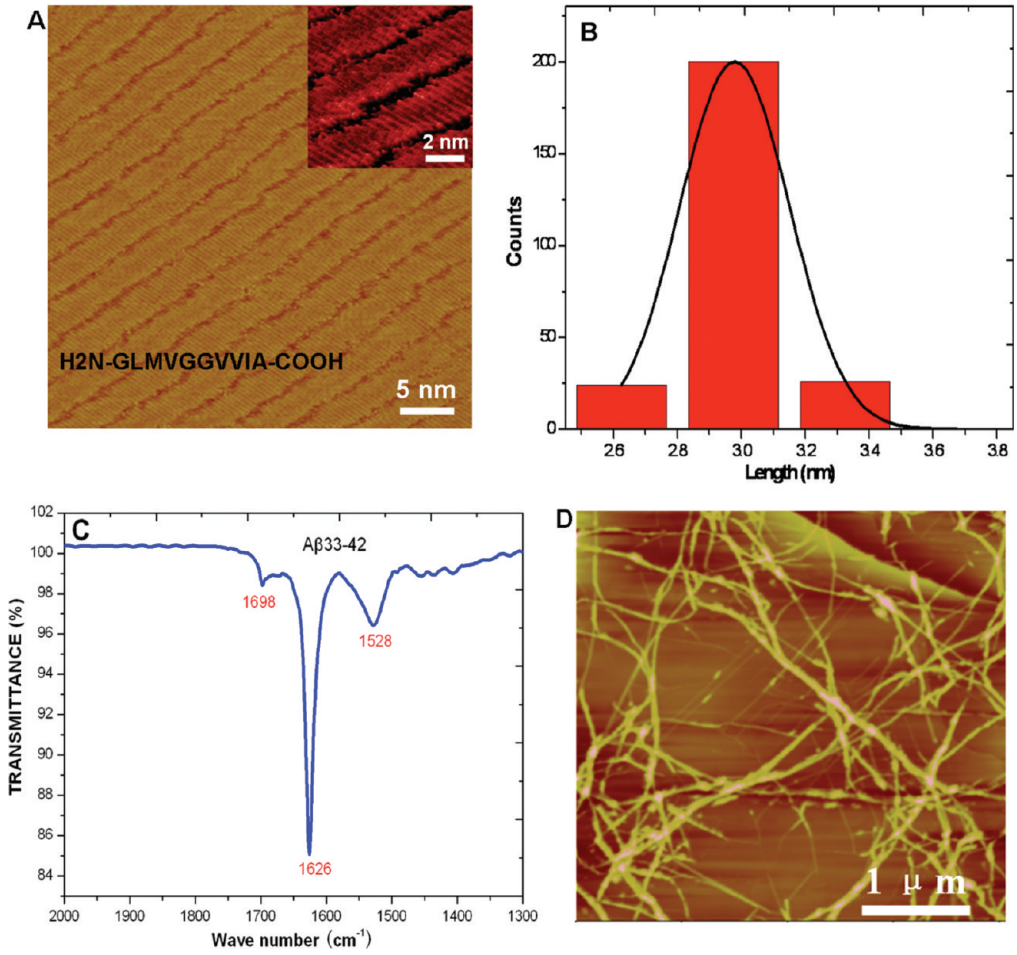

Figure 1. (A) STM images of two-dimensional assemblies of Aβ33−42 on HOPG surface. The inset image at the upper right corner is high resolution 3D STM image of Aβ33−42. The amino acid sequence of Aβ33−42 is imposed on the STM image in (A). The tunneling conditions are (A) 799 mV and 299 pA, 500 mV and 299 pA (inset). (B) The histogram of chain length values with Gaussian fitting for Aβ33−42. (C) FTIR spectrum of Aβ33−42. (D) The AFM image of Aβ33−42 aggregates.

semblies. The results could be beneficial for understanding the interstacking interactions as well as for developing therapeutical approaches.[34,35] STM and AFM (Nanoscope IIIa system, Vecco, Metrology group, U.S.A.) were used for investigating the characteristics of Aβ33−42 assemblies, the aggregation morphology of the peptides, and the modulator effect on Aβ33−42 assemblies on the surface of highly oriented pyrolytic graphite (HOPG). The secondary structures of Aβ33−42 assemblies were detected by Fourier transform infrared (FTIR) spectroscopy (Perkin Elmer Fourier transform infrared spectrometer at a resolution of 4 cm^{-1} in the transmission mode with BaF_2 windows). Furthermore, the chaperone-like modulator effect on promoting peptide aggregation was explored in aqueous solution by using light scattering method (Perkin Elmer LS55 fluorescence spectrophotometer at room temperature using 1 cm path length quart cell).

Initially, the self-assembly structures of the beta-amyloid peptide assemblies of Aβ33−42 are observed by STM on HOPG surface with molecular level resolution. The assembly of the peptide Aβ33−42 (H_2N-GLMVGGVVIA-COOH) is illustrated in the STM image in Figure 1A. The Aβ33−42 contains 10 amino acids and most of them are nonpolar amino acids. It has also been proposed that the amino acids from 29 to 42 in Aβ42 are considered important for the aggregation of Aβ42, since this fragment is the core structure of the Aβ42 hairpin and also plays important role in the formation of beta-sheet structure owing to the hydrophobicity of the amino acids.[35−37] Moreover, this fragment may contribute to the cytotoxicity of the peptide by destabilizing cell membranes.[35−37] Therefore, it is of genuine interest to study the aggregation characteristics of these peptide fragments of Aβ42. Figure 1A is a large area STM image of the assemblies of Aβ33−42 on HOPG surface. The structural characteristics of the assembly are similar to that of Aβ42.[33] The distance between two neighboring chains is estimated to be 0.45 ± 0.01 nm, which is consistent with the expected separation between two neighboring peptides with beta-sheet secondary structures.[21,24,38,39] The high resolution STM image of Aβ33−42 is shown at the upper right of Figure 1A. The above measurements of the apparent width of the peptide lamellae suggest that the peptides are assembled in extended form rather than hairpin structures. The distribution of the peptide length is shown in Figure 1B and also listed in Supporting Information, Table S1. One can recognize that the measured lengths of Aβ33−42 range from 2.80 to 3.15 nm, which correspond to the length of a peptide consisting of 9 amino acids. Considering the experimental uncertainty

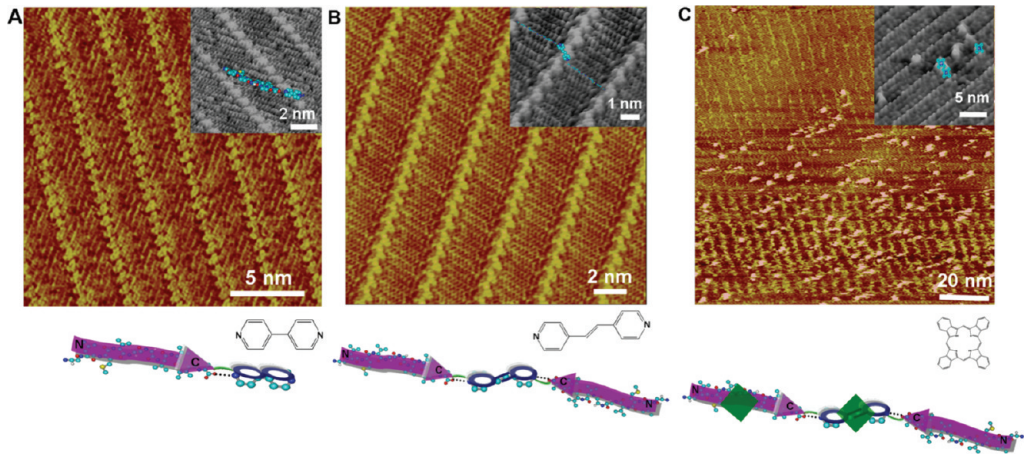

Figure 2. The STM images of modulated Aβ33−42 assembly structures of (A) Aβ33−42/DP, (B) Aβ33−42/DPE, (C) Aβ33−42/DPE/Pc. The inset images at the upper right corners are high resolution 3D STM images of the corresponding peptide-modulator complex assemblies. The imaging conditions are (A) 729 mV and 443 pA, 729 mV and 443 pA (inset); (B) 700 mV and 417 pA, 630 mV and 522 pA (inset); (C) 1165 mV and 163 pA, 1062 mV and 212 pA (inset). The proposed basic building block models for the peptide-modulator complex assemblies in lower panel of (A) Aβ33−42/DP, (B) Aβ33−42/DPE, (C) Aβ33−42/DPE/Pc. The purple arrows stand for the beta strands, the blue circles are for the pyridyl rings, and the green squares are for the Pc molecules. The molecular structures of 4,4-bipyridyl (DP), 1,2-di(4pyridyl)ethylene (DPE), and phthalocyanine (Pc) are provided in (A−C).

associated with identifying the terminal amino acids, we believe that the chain lengths of Aβ33−42 from the STM observation is consistent with the expected one of Aβ33−42 with antiparallel beta-sheet secondary structures as revealed by FTIR results shown in Figure 1C. The presence of the two bands in FTIR spectra, namely the major one at 1626 cm^{-1} and the minor one at 1698 cm^{-1} are characteristic of an antiparallel beta-sheet of the peptide assembly.[28,29,40] The above results are qualitatively consistent with the previously proposed model of amyloid fibrils Aβ34−42 in antiparallel arrangement based on solid-state NMR results.[25] The morphologies of the Aβ34−42 aggregates are fibrils as shown in Figure 1D. The height and width of the fibrils are approximately 7 and 70 nm from AFM measurements as shown in Supporting Information, Figure S1A,B.

It has been reported that molecules could interact with beta-amyloid peptides resulting in inhibition effects on peptide aggregations.[41,42] It is therefore interesting to study the interaction mechanisms between molecules and beta-amyloid proteins. In the present study, two organic molecules, 4,4-bipyridyl (DP) and 1,2-di(4pyridyl)ethylene (DPE), were used as the chaperone-like terminus modulators to interact with the beta amyloid fragment peptide Aβ33−42.

The STM image for Aβ33−42/DP assembly structure shown in Figure 2A reveals the lamella characteristics with DP molecular arrays between two Aβ33−42 stripes. The molecular structure of DP is shown in the lower panel of Figure 2A. The 3D illustration of the peptide-modulator assembly structure of Aβ33−42/DP is presented as an inset at the upper right of Figure 2A. The schematic model of the terminus modulating effect is illustrated at the bottom of Figure 2A. The hydrogen-bond interaction between the nitrogen atoms of DP and the −COOH group of peptide C terminus is deterministic to the modulated peptide assembly, which is similar to that found previously in the heterogeneous assemblies of DP and stearic acids.[43] The width of the bright features associated with DP molecules is 0.73 nm, which is consistent with the size of the DP in STM observations.[43] The average width of the peptide chain is about 3.48 nm. Considering the terminal carboxyl and amino groups the measured length is approximately consistent with the expected length of Aβ33−42.[25] (The repeat distance per residue is 0.35 nm expected in an antiparallel β-sheet secondary structure. Therefore the expected length of Aβ33−42 consisting of 10 amino acids is 3.15 nm (0.35 nm × 9 = 3.15 nm).)[44]

The modulating effect of DPE molecule on Aβ33−42 peptide assembly is revealed in Figure 2B and the schematic model of DPE modulating effect is presented in the lower panel of Figure 2B. Similar to the heterogeneous assemblies of Aβ33−42/DP, the C terminus of Aβ33−42 interacts with DPE via N...H−O hydrogen bond. However, the building block of Aβ33−42/DPE is different from that of Aβ33−42/DP. It is evident that one chaperone-like modulator of DPE is accompanied by two peptides. This phenomenon could be ascribed to the *trans*-conformation of the DPE molecules that originated from the ethylene groups between two pyridyl groups. The length of the DPE molecule determined from the STM image is approximately 0.9 nm, which is a little larger than that of DP (0.73 nm), due to the extra ethylene group in DPE molecule. The length of peptide determined from the STM image is approximately consistent with the expected value mentioned above.

It can be observed from the above results that there are some common features between the two modulators in modulating the peptide assemblies. The driving forces of the two modulating effects are identical. From the peptide/DP and peptide/DPE unit cells (Supporting Information, Figure S2A,B), the discrepancy can be identified between the two modulators comprised of two aspects, ratios of peptides and modulators (1:1 for DP and 2:1 for DPE) and the angles of the unit cells (42° for DP and 72° for DPE). The attachment

of the ethylene group between the two pyridyls in DPE enhances the flexibility of DPE in comparison to that of DP molecules, which could enable the hydrogen bond interaction between two peptides and one DPE molecules via two N atoms in pyridyl groups. The observed different angles between the two unit cells can be attributed to the trans-conformation of the DPE molecular modulators. This result indicates the importance of the structural effects in modulating the assembly process of peptides by chaperone-like terminus modulators.

Side group interaction is also keen to the aggregation of peptides via van der Waals interaction and hydrophobic interaction. An organic molecule, phthalocyanine (Pc) was introduced to study its interaction with the side groups of Aβ33−42 together with the terminus modulators.

The DPE was used to label the peptide Aβ33−42 while Pc was introduced simultaneously to the peptide assembly. Figure 2C presents the STM image for Aβ33−42/DPE/Pc complex and the molecular structure of Pc is shown in the lower panel of this figure. It can be recognized that the Pc molecules are immobilized on top of the heterogeneous Aβ33−42/DPE lamella structure. A 3D high resolution STM image of Aβ33−42/DPE/Pc complex is displayed at the upper right of Figure 2C. The Pc monomers and oligomers are stacked on the peptide chains or DPE molecules. The schematic model at the bottom of Figure 2C illustrates the proposed Pc adsorption structure. The Pc molecules are adsorbed to the peptide chain possibly via hydrophobic interactions between the hydrophobic residues of peptides and aromatic moieties of Pc. In addition, the adsorption of Pc on DPE modulators could be dominated by $\pi-\pi$ interactions of DPE and PC. The side widths of the single molecule Pcs (Supporting Information, Figure S1C) were measured to be 1.35 or 1.46 nm, which are consistent with the previous reports.[45,46]

The above STM observations demonstrate that chaperone-like modulators could regulate the assembly process of the Aβ33−42 on molecular level. In parallel studies, AFM investigations were conducted for studying the modulator effects on the morphology of the peptide aggregates. The AFM image of Aβ33−42 aggregates (Figure 1D) deposited on HOPG surface clearly shows the fibril structures. The AFM images in Figure 3A,B demonstrate predominantly films rather than fibrils for the aggregates of Aβ33−42 mixed with chaperone-like terminus modulators, DP and DPE respectively. The AFM images of Aβ33−42/DPE/Pc and Aβ33−42/Pc complexes shown in Figure 3C,D clearly illustrate film-like topography together with evenly distributed particulates rather than fibrils. The dependency of the aggregate morphology on modulators indicates the possibility of regulating Aβ assembly structures with different molecular modulators.

The FTIR results could provide the information about the secondary structure of the peptide assembly regulated by modulators. Figure 4 presents the FTIR spectra of Aβ33−42, DPE, DP, Aβ33−42/DPE, Aβ33−42/DP complexes. The peak signals of the major bands at 1597 cm^{-1}, minor bands at 1556 cm^{-1}, and 1416 cm^{-1} are attributed to the traits of

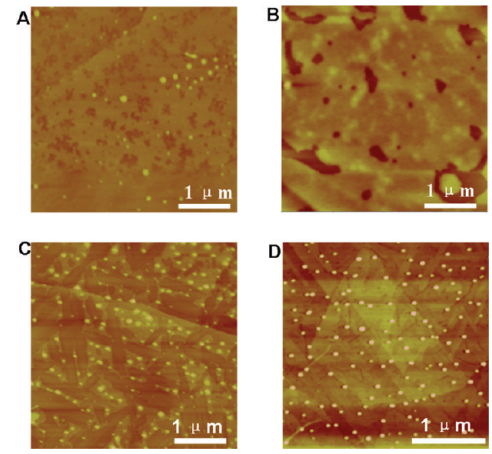

Figure 3. The AFM images of aggregates of Aβ33−42 with chaperone-like peptide-modulator aggregates on HOPG surface. (A) Aβ33−42/DP, (B) Aβ33−42/DPE, (C) Aβ33−42/DPE/Pc, and (D) Aβ33−42/Pc on HOPG surface. The *z*-scales for all the images are 20 nm.

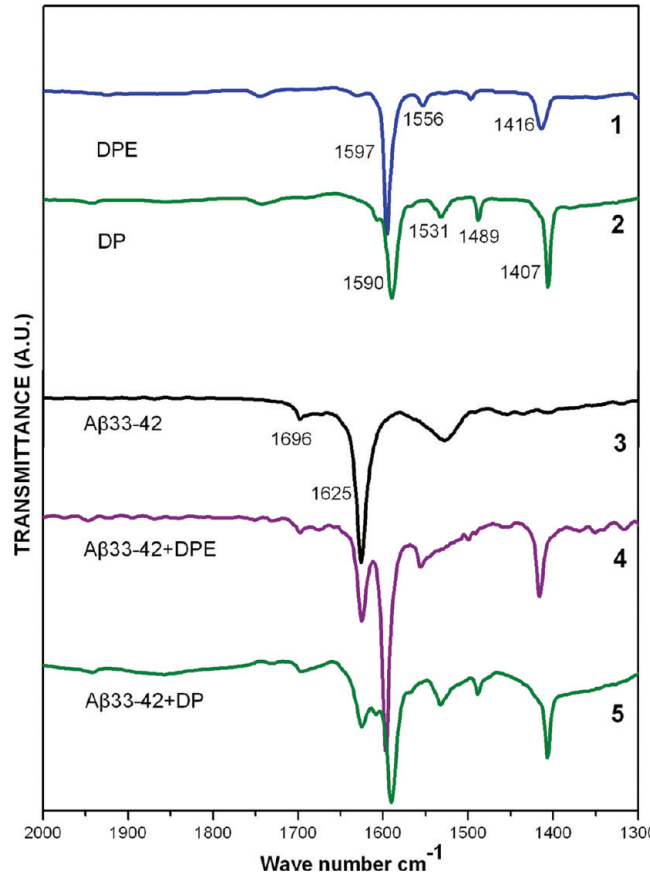

Figure 4. FTIR spectra of DPE (1), DP (2), Aβ33−42 (3), Aβ33−42/DPE (4), and Aβ33−42/DP (5) systems. The characteristic bands of DPE, DP, and Aβ33−42 have been labeled in the spectra.

DPE; the bands at 1590, 1531, 1489, and 1407 cm^{-1} are characteristics for DP, which are revealed in Curve 1 and Curve 2 of Figure 4. The presence of the two bands, the major one at 1626 cm^{-1} and the minor one at 1698 cm^{-1}, indicates the presence of an antiparallel beta conformation of the peptide aggregates as shown in Curve 3 of Figure 4.[28,29,40] There is another significant feature at 1525 cm^{-1},

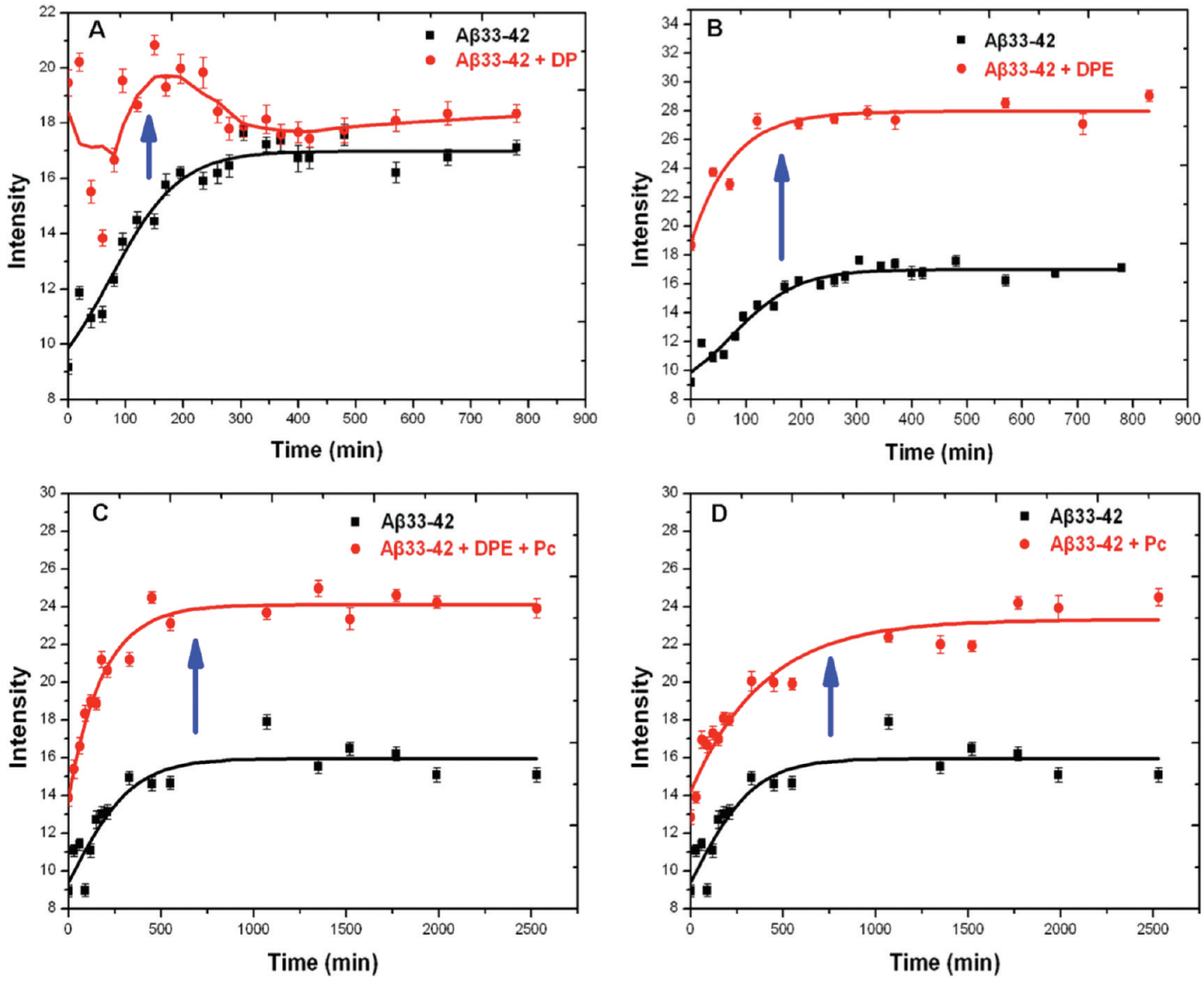

Figure 5. Modulating effects of terminus modulators (A) DP, (B) DPE and side group modulators (C) DPE + Pc, (D) Pc on the aggregation of Aβ33−42 in aqueous solution as measured by light scattering. The legends are shown in panels A−D, respectively. The red and black solid lines are presented just for guiding the eyes. The blue arrows indicate the accelerating effect of peptide aggregation in the presence of modulators.

which can be attributed to the amide II vibration of the peptides.[40] The FTIR spectra of the peptide complex assemblies in Curves 4 and 5 in Figure 4 reveal that the characteristic features of the peptide Aβ33−42 are retained in the Aβ33−42/DP and Aβ33−42/DPE complexes. The spectrum features of the complexes demonstrate the simple overlapping of both the peptides and the terminus modulators, which are indicative of negligible effects of the modulators on the antiparallel secondary structures of Aβ33−42.

To assess the impact of the stimulated molecular chaperones approach toward modulating peptide aggregation in aqueous solution, Aβ33−42 and Aβ33−42 in the presence of modulators were incubated and the aggregation was tracked by turbidity measurements. It can be readily observed that the introduction of modulators could appreciably accelerate the aggregation of peptide Aβ33−42 in aqueous solution as shown in Figure 5A−D. The light scattering results reveal that terminus modulator DPE has higher impact in comparison to that of DP on promoting the aggregation of Aβ33−42 in Figure 5A,B. It is possibly attributed to the different ratios between peptide and modulators revealed in STM investigations (Figure 2A,B), that is, one DPE molecule can interact with two peptides while one DP molecule can only interacts with one peptide. The similar modulating effect on aggregation of Aβ33−42 was observed for the side group modulators of Pc as shown in Figure 5C,D. Dramatic increase could be observed in the light scattering intensity in the presence of DPE/Pc or Pc. Considering the similar results for both side group modulators and terminus group modulators, it is therefore plausible to suggest that both of these two kinds of modulators would serve as regulating reagents for accelerating the aggregation of peptide Aβ33−42.

It should be noted that a number of reports have suggested that the neuron toxicity is caused by the oligomers of beta-amyloid peptide rather than the mature fibrils.[6,47,48] The chaperone-like modulators introduced in this work could accelerate the peptide aggregation in aqueous solutions, which could be beneficial for exploring venues of reducing the neuron toxicity by accelerating the aggregation process of beta amyloid peptides.

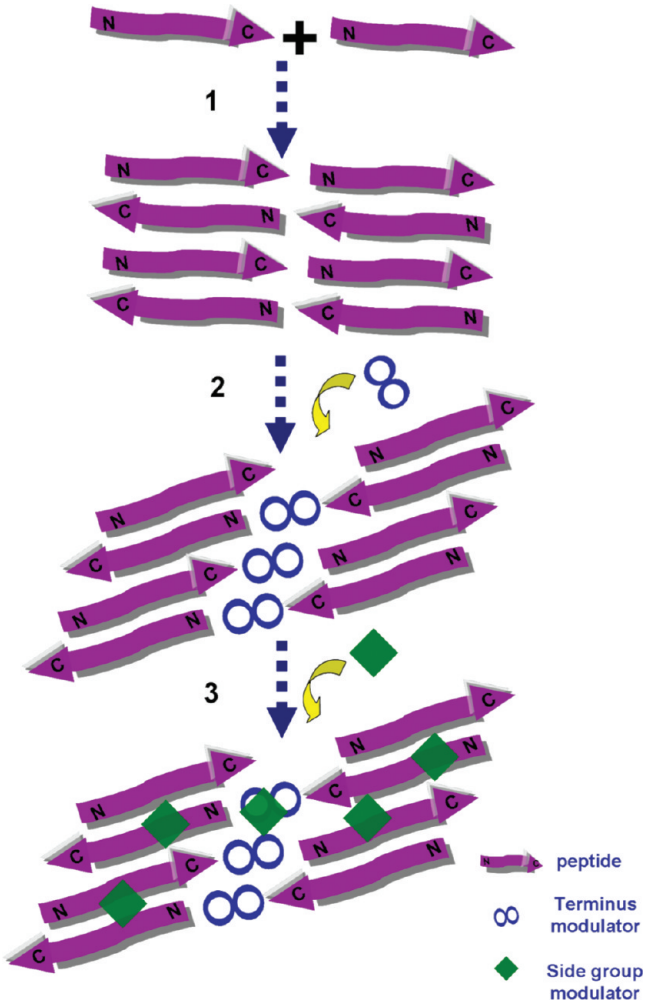

Figure 6. The schematic illustration of the chaperone-like modulators affecting the aggregation of peptides.

On the basis of the above results, a schematic illustration is proposed in Figure 6 showing the effect of chaperone-like modulators on the aggregation of the peptide. The peptides aggregate to the lamella assemblies with antiparallel β-sheets secondary structures via intermolecular hydrogen bond and hydrophobic interaction as shown in Illustration 1 of Figure 6. In the presence of the terminus molecular modulators, they could regulate the assembling behaviors of the peptides as revealed in Illustration 2 of Figure 6. The interactions of the peptide termini possibly have been interfered by modulators resulting in a complex assembly of peptide/modulator via hydrogen bond between the C termini of the peptides and N atoms of modulators. On the basis of the supramolecular assembly structures of peptide/terminus modulator, the side group modulator is introduced to further regulate the peptide assembly by adsorbing onto the peptide chains or terminus modulators via hydrophobic interactions or $\pi-\pi$ interactions. The process is presented in Illustration 3 of Figure 6, which suggests that the side group modulators are likely to mediate the interaction between two peptide lamellas and subsequently accelerate the aggregation of peptides.

In summary, the chaperone-like modulator effects on Aβ33−42 peptide aggregation have been investigated by using STM, AFM, and FTIR at liquid−solid interface and by using light scattering in aqueous solution. The experimental results suggest that the STM method could provide useful insights into the assembly behaviors of the peptide aggregates at liquid−solid interface on molecular level. The modulator effect of peptide assemblies are demonstrated both for the surface assembling processes and aggregation in solution. Such observations on the modulator effect could provide effective approach toward modulating Aβ peptide aggregation via diversity of interactions such as hydrogen bond, hydrophobic interaction, etc. It could be also beneficial for potential drug designs relating to neurodegenerative diseases.

Acknowledgment. This work was supported by the National Basic Research Program of China (2009CB930100) and National Natural Science Foundation of China (20911130229). Financial support from CAS Key Laboratory of Nano Bioeffect and Biosafety is also gratefully acknowledged.

Supporting Information Available: This material is available free of charge via the Internet at http://pubs.acs.org.

References

(1) Shastry, B. S. Neurodegenerative disorders of protein aggregation. *Neurochem. Int.* **2003**, *43*, 1.
(2) Roberson, E. D.; Mucke, L. 100 years and counting: prospects for defeating Alzheimer's disease. *Science* **2006**, *314*, 781.
(3) Goedert, M.; Spillantini, M. G. A century of Alzheimer's disease. *Science* **2006**, *314*, 777.
(4) Brody, D. L.; Magnoni, S. Amyloid-β dynamics correlate with neurological status in the injured human brain. *Science* **2008**, *321*, 1221.
(5) Makin, O. S.; Serpell, L. C. Structures for amyloid fibrils. *FEBS. J.* **2005**, *272*, 5950.
(6) Lambert, M. P.; Klein, W. L. Diffusible, nonfibrillar ligands derived from Aβ1−42 are potent central nervous system neurotoxins. *Proc. Natl. Acad. Sci. U.S.A.* **1998**, *95*, 6448.
(7) Lashuel, H. A.; Hartley, D.; Petre, B. M.; Walz, T.; Lansbury, P. T. Amyloid pores from pathogenic mutations. *Nature* **2002**, *418*, 291.
(8) Quist, A.; Doudevski, I.; Lal, R. Amyloid ion channels: A common structural link for protein-misfolding disease. *Proc. Natl. Acad. Sci. U.S.A.* **2005**, *102*, 10427.
(9) Irie, K.; Murakami, K.; Masuda, Y. Structure of beta-amyloid fibrils and its relevance to their neurotoxicity: implications for pathogenesis of Alzheimer's disease. *J. Biosci. Bioeng.* **2005**, *99*, 437.
(10) Kirschner, D. A.; Inouye, H.; Duffy, L. K.; Sinclair, A.; Lind, M.; Selkoe, D. J. Synthetic peptide homologous to beta-protein from Alzheimer-disease forms amyloid-like fibrils in vitro. *Proc. Natl. Acad. Sci. U.S.A.* **1987**, *84*, 6953.
(11) Mikros, E.; Benaki, D.; Humpfer, E.; Spraul, M.; Loukas, S.; Stassinopoulou, C. I.; Pelecanou, M. High-resolution NMR spectroscopy of the beta-amyloid(1−28) fibril typical for Alzheimer's disease. *Angew. Chem., Int. Ed.* **2001**, *40*, 3603.
(12) Pike, C. J.; Burdick, D.; Walencewicz, A. J.; Glabe, C. G.; Cotman, C. W. Neurodegeneration induced by beta-amyloid peptides invitro - the role of peptide assembly state. *J. Neurosci.* **1993**, *13*, 1676.
(13) Behl, C.; Davis, J. B.; Lesley, R.; Schubert, D. Hydrogen-peroxide mediates amyloid-beta protein toxicity. *Cell* **1994**, *77*, 817.
(14) Shearman, M. S.; Ragan, C. I.; Iversen, L. L. Inhibition of Pc12 cell redox activity is a specific, early indicator of the mechanism of beta-amyloid-mediated cell-death. *Proc. Natl. Acad. Sci. U.S.A.* **1994**, *91*, 1470.
(15) Lorenzo, A.; Yankner, B. A. Beta-amyloid neurotoxicity requires fibril formation and is inhibited by Congo red. *Proc. Natl. Acad. Sci. U.S.A.* **1994**, *91*, 12243.
(16) Kang, J.; Lemaire, H. G.; Unterbeck, A.; Salbaum, J. M.; Masters, C. L.; Grzeschik, K. H.; Multhaup, G.; Beyreuther, K.; Mullerhill, B. The precursor of Alzheimers-disease amyloid-A4 protein resembles a cell-surface receptor. *Nature* **1987**, *325*, 733.
(17) Masters, C. L.; Simms, G.; Weinman, N. A.; Multhaup, G.; McDonald, B. L.; Beyreuther, K. Amyloid plaque core protein in Alzheimer-

disease and down syndrome. *Proc. Natl. Acad. Sci. U.S.A.* **1985**, *82*, 4245.
(18) Westlind-Danielsson, A.; Arnerup, G. Spontaneous in vitro formation of supramolecular beta-amyloid structures, "beta amy balls", by beta-amyloid 1−40 peptide. *Biochemistry* **2001**, *40*, 14736.
(19) Selenica, M. L.; Wang, X.; Ostergaard-Pedersen, L.; Westlind-Danielsson, A.; Grubb, A. Cystatin C reduces the in vitro formation of soluble A beta 1−42 oligomers and protofibrils. *Scand. J. Clin. Lab. Invest.* **2007**, *67*, 179.
(20) Lau, T. L.; Ambroggio, E. E.; Tew, D. J.; Cappai, R.; Masters, C. L.; Fidelio, G. D.; Barnham, K. J.; Separovic, F. Amyloid-beta peptide disruption of lipid membranes and the effect of metal ions. *J. Mol. Biol.* **2006**, *356*, 759.
(21) Petkova, A. T.; Ishii, Y.; Balbach, J. J.; Antzutkin, O. N.; Leapman, R. D.; Delaglio, F.; Tycko, R. A structural model for Alzheimer's beta-amyloid fibrils based on experimental constraints from solid state NMR. *Proc. Natl. Acad. Sci. U.S.A.* **2002**, *99*, 16742.
(22) Tycko, R. Molecular structure of amyloid fibrils: insights from solid-state NMR. *Q. Rev. Biophys.* **2006**, *39*, 1.
(23) Malinchik, S. B.; Inouye, H.; Szumowski, K. E.; Kirschner, D. A. Structural analysis of Alzheimer's beta(1−40) amyloid: protofilament assembly of tubular fibrils. *Biophys. J.* **1998**, *74*, 537.
(24) Serpell, L. C.; Blake, C. C. F.; Fraser, P. E. Molecular structure of a fibrillar Alzheimer's A beta fragment. *Biochemistry.* **2000**, *39*, 13269.
(25) Lansbury, P. T.; Costa, P. R.; Griffiths, J. M.; Simon, E. J.; Auger, M.; Halverson, K. J.; Kocisko, D. A.; Hendsch, Z. S.; Ashburn, T. T.; Spencer, R. G. S.; Tidor, B.; Griffin, R. G. Structural model for the beta-amyloid fibril based on interstrand alignment of an antiparallel-sheet comprising a C-terminal peptide. *Nat. Struct. Biol.* **1995**, *2*, 990.
(26) Nelson, R.; Sawaya, M. R.; Balbirnie, M.; Eisenberg, D. Structure of the cross-β spine of amyloid-like fibrils. *Nature* **2005**, *435*, 773.
(27) Sawaya, M. R.; Sambashivan, S.; Nelson, R.; Eisenberg, D. Atomic structures of amyloid cross-β spines reveal varied steric zippers. *Nature* **2007**, *447*, 453.
(28) Hilbich, C.; Kisters-Woike, B.; Reed, J.; Masters, C. L.; Beyreuther, K. Aggregation and secondary structure of synthetic amyloid βA4 peptides of Alzheimer's disease. *J. Mol. Biol.* **1991**, *218*, 149.
(29) Matsuzaki, K.; Horikiri, C. Interactions of amyloid β-peptide (1−40) with ganglioside-containing membranes. *Biochemistry* **1999**, *38*, 4137.
(30) Kudernac, T.; Lei, S. B.; Elemans, J. A. A. W.; De Feyter, S. Two-dimensional supramolecular self-assembly: nanoporous networks on surface. *Chem. Soc. Rev.* **2009**, *38*, 402.
(31) Barth, J. V.; Costantini, G.; Kern, K. Engineering atomic and molecular nanostructures at surfaces. *Nature* **2005**, *437*, 671.
(32) Lingenfelder, M.; Tomba, G.; Costantini, G.; Ciacchi, L. C.; De Vita, A.; Kern, K. Tracking the chiral recognition of adsorbed dipeptides at the single-molecule level. *Angew. Chem., Int. Ed.* **2007**, *46*, 4492.
(33) Ma, X. J.; Liu, L.; Mao, X. B.; Niu, L.; Deng, K.; Wu, W. H.; Li, Y. M.; Yang, Y. L.; Wang, C. Amyloid-β (1−42) folding multiplicity and single molecule binding behavior studied by STM. *J. Mol. Biol.* **2009**, *388*, 894.
(34) Soto, C.; Sigurdsson, E. M.; Morelli, L.; Kumar, R. A.; Castano, E. M.; Frangione, B. Beta-sheet breaker peptides inhibit fibrillogenesis in a rat brain model of amyloidosis: implications for Alzheimer's therapy. *Nat. Med.* **1998**, *4*, 822.
(35) Mingeot-Leclercq, M. P.; Lins, L.; Bensliman, M.; Van Bambeke, F.; van der Smissen, P.; Peuvot, J.; Schanck, A.; Brasseur, R. Membrane destabilization induced by beta-amyloid peptide 29−42: importance of the amino-terminus. *Chem. Phys. Lipids.* **2002**, *120*, 57.
(36) Itoh, S. G.; Okamoto, Y. Amyloid-β (29−42) dimer formations studied by a multicanonical-multioverlap molecular dynamics simulation. *J. Phys. Chem. B* **2008**, *112*, 2767.
(37) Demeester, N.; Baier, G.; Enzinger, C.; Goethals, M.; Vandekerckhove, J.; Rosseneu, M.; Labeur, C. Apoptosis induced in neuronal cells by C-terminal amyloid beta-fragments is correlated with their aggregation properties in phospholipid membranes. *Mol. Membr. Biol.* **2000**, *17*, 219.
(38) Arimon, M.; Diez-Perez, I.; Kogan, M. J.; Durany, N.; Giralt, E.; Sanz, F.; Fernandez-Busquets, X. Fine structure study of A beta(1−42) fibrillogenesis with atomic force microscopy. *FASEB J.* **2005**, *19*, 1344.
(39) Kowalewski, T.; Holtzman, D. M. In situ atomic force microscopy study of Alzheimer's beta-amyloid peptide on different substrates: new insights into mechanism of beta-sheet formation. *Proc. Natl. Acad. Sci. U.S.A.* **1999**, *96*, 3688.
(40) Miyazawa, T.; Blout, E. R. Infrared spectra of polypeptides in various conformations - amide I and II bands. *J. Am. Chem. Soc.* **1961**, *83*, 712.
(41) Gestwicki, J. E.; Crabtree, G. R.; Graef, I. A. Harnessing chaperones to generate small-molecule inhibitors of amyloid beta aggregation. *Science.* **2004**, *306*, 865.
(42) Ono, K.; Naiki, H.; Yamada, M. The development of preventives and therapeutics for Alzheimer's disease that inhibit the formation of beta-amyloid fibrils (fA beta), as well as destabilize preformed fA beta. *Curr. Pharm. Design.* **2006**, *12*, 4357.
(43) Xu, B.; Yin, S. X.; Wang, C.; Zeng, Q. D.; Qiu, X. H.; Bai, C. L. Identification of hydrogen bond characterizations of isomeric 4Bpy and 2Bpy by STM. *Surf. Interface Anal.* **2001**, *32*, 245.
(44) Pauling, L.; Corey, R. B. Two rippled-sheet configurations of polypeptide chains, and a note about the pleated sheets. *Proc. Natl. Acad. Sci. U.S.A.* **1953**, *39*, 253.
(45) Lei, S. B.; Wang, C.; Wan, L. J.; Bai, C. L. Site selective adsorption and templated assembling: effect of organic-organic heterogeneous interface studied by scanning tunneling microscopy. *J. Phys. Chem. B* **2004**, *108*, 1173.
(46) Lei, S. B.; Deng, K.; Yang, Y. L.; Zeng, Q. D.; Wang, C.; Jiang, J. Z. Electic driven molecular switching of asymmetric tris(phthalocyaninato) lutetium tirple-decker complex at the liquid/solid interface. *Nano Lett.* **2008**, *8*, 1836.
(47) Klein, W. L. Aβ toxicity in Alzheimer's disease: globular oligomers (ADDLs) as new vaccine and drug targets. *Neurochem. Int.* **2002**, *42*, 345.
(48) De Felice, F. G.; Velasco, P. T.; Lambert, M. P.; Viola, K.; Fernandez, S. J.; Ferreira, S. T.; Klein, W. L. Aβ oligomers induce neuronal oxidative stress through an N-Methyl-D-aspartate receptor-dependent mechanism that is blocked by the Alzheimer drug memantine. *J. Bio. Chem.* **2007**, *282*, 11590.

NL902256B